

# Fault-Tolerant Postselected Quantum Computation: Threshold Analysis

E. Knill\*

*Mathematical and Computational Sciences Division,  
National Institute of Standards and Technology, Boulder CO 80305*

(Dated: October 22, 2018)

The schemes for fault-tolerant postselected quantum computation given in [Knill, Fault-Tolerant Postselected Quantum Computation: Schemes, <http://arxiv.org/abs/quant-ph/0402171>] are analyzed to determine their error-tolerance. The analysis is based on computer-assisted heuristics. It indicates that if classical and quantum communication delays are negligible, then scalable qubit-based quantum computation is possible with errors above 1 % per elementary quantum gate.

## I. INTRODUCTION

In [1] a scheme for fault-tolerant postselected quantum computation based on concatenating four-qubit error-detecting codes is presented. Here, the error behavior of the scheme is analyzed with the help of computer-assisted heuristics and shown to tolerate errors above 1 % per elementary quantum gate. This result generalizes to standard quantum computation because fault-tolerant postselected quantum computation can be used for preparing stabilizer states with well constrained local errors. With this technique, any sufficiently error-tolerant stabilizer code can be used with teleported error correction [2] to realize a general fault-tolerant computation. In particular, the analysis indicates that the error threshold for scalable quantum computation is also above 1 %. This substantially improves thresholds obtained previously, both heuristically and by proof [3, 4, 5, 6, 7, 8, 9, 10, 11, 12, 13, 14, 15, 16, 17, 18, 19, 20, 20, 21, 22].

The analysis given below assumes familiarity with the previous two papers in the series [1, 2]. See [2] for motivation, background, and a brief review of the needed stabilizer code theory and teleported error correction. For details of the scheme analyzed here see [1].

The following conventions are used: A *postselected computation* is one whose output is conditional on the outcomes of measurements of ancilla qubits used during the computation. The usual model of quantum computation is referred to as *standard* quantum computation. A scheme for fault-tolerant computation starts with *physical qubits* and an error model for a universal set of quantum gates (including measurement and state preparation). The schemes discussed here involve the construction of *logical qubits* to be used in a general-purpose computation. Logical qubits are manipulated with *logical gates*. The construction involves one or more levels of encoding, each of which defines higher-level logical qubits in terms of lower-level ones. In a given context, the term “logical” refers to the highest-level logical qubits currently being discussed. The terms *encoded qubit*, *encoded state* and *encoded gate* are used to refer to encoded quantum information if the emphasis is on the code used rather than on logical computation. The most important state used for implementing fault tolerance is the encoded Bell pair. This state consists of two encoded qubits in the standard Bell state,  $\frac{1}{\sqrt{2}}(|00\rangle + |11\rangle)$ . Thus, there are two blocks of physical

---

\*knill@boulder.nist.gov

qubits, one for each encoded qubit. The two blocks and their encoded qubits are referred to as the *origin* and *destination* blocks and qubits, respectively. The Bell pairs are used in teleportation by making a transversally implemented Bell measurement on the block to be teleported and on the origin block. Most of the states under consideration are  $n$ -qubit stabilizer states characterized by an  $n \times 2n$  binary generator matrix whose rows specify a generating set of stabilizing Pauli products. Errors in the state are characterized by the *syndrome*, a binary  $n$ -vector that specifies the eigenvalues of the stabilizing Pauli products. The error-free state is standardized to have a syndrome (vector) of  $\mathbf{0}$ . When talking about encoded qubits, the generator matrix has fewer than  $n$  rows. The syndrome specifies the eigenvalues of the Pauli products determined by the rows of the generator matrix. The following abbreviations are used:  $X = \sigma_x$ ,  $Z = \sigma_z$ ,  $Y = \sigma_x \sigma_z$ . The states  $|0\rangle$ ,  $|+\rangle$  and  $|i\pi/4\rangle$  are, respectively, the  $+1$  eigenstates of  $Z$ ,  $X$  and  $iY$ .  $|\pi/8\rangle$  is the  $+1$  eigenstate of the Hadamard gate.

## II. ASSUMPTIONS

As is customary for theoretical threshold analyses, it is assumed that it is possible to apply quantum gates in a parallel fashion without geometrical constraints. In particular, in each time step, any pair of qubits can be acted on with a controlled not (cnot) gate (no quantum communication latency), and all qubits may be involved in a non-trivial operation. All gates (one-qubit state preparations, Hadamard gates, cnots, one-qubit measurements) are assumed to take the same amount of time. As discussed in [1], for the postselected computation scheme used here, gate times can vary between gate types. In particular, the time needed for a measurement may be longer than that for the cnot. Variations in gate time have an effect only when prepared states are used in a standard quantum computation, where an additional memory error may need to be accounted for. It is assumed that classical computation based on measurement outcomes is instantaneous and error-free (no classical communication or computation latency). This condition is needed when prepared states are to be used for standard quantum computation, as it is necessary to determine whether all postselection criteria have been met and (for efficient postselection) what the current syndrome is for the prepared state.

The error model used here is based on having all errors be probabilistic Pauli products acting independently at error locations associated with each gate. Specifically, a quantum computation is described in terms of its quantum network. Each instance of a given quantum computation is modified by probabilistically inserting Pauli operators after each network element and before measurements. To describe the constraints on the probabilities, an *error location* is associated with each network element. For a state-preparation and the Hadamard gate, the error location is in the qubit line immediately following the state-preparation gate. For the cnot, it extends to both qubit lines immediately after the gate. For measurements, it is on the qubit to be measured just before the gate. For each Pauli operator  $p$  (or product of two Pauli operators in the case of the cnot) that can act at an error location  $l$ , there is an associated error parameter  $e_{p,l}$ . The strongest assumption one can make is that errors are probabilistic and independent between locations, with  $e_{p,l}$  the probability that  $p$  acts at location  $l$ .

The heuristic used for the analysis involves a method that uses an independent-error model to approximate the error behavior in prepared states. This method is used at each level of a concatenation procedure. Given independence at the lower level, the true error behavior is close to, but not exactly, independent. Ideally, the independent-error model used should not underestimate any error probabilities after postselection. The motivation for using such an independent approximation comes from a classification of error models that retain some of the crucial properties of

independence. In particular, the independence assumption can be weakened in three steps. Consider sets of error locations  $L$  and  $K$  with  $|L| + 1 = |K|$ , such that there is an injection  $\pi$  from locations in  $L$  to equivalent locations in  $K$ . Locations are considered equivalent if they are associated with identical gates. Let  $r$  be the location in  $K$  not in the image of  $\pi$ . Let  $p_l$  and  $q_k$  be (non-identity) Pauli operators acting at locations  $l \in L$  and  $k \in K$ , respectively, with the property  $q_{\pi(l)} = p_l$ . The error model is independent( $A$ ) if it is always the case that the relative probability  $\text{Prob}(\prod_{k \in K} q_k) / \text{Prob}(\prod_{l \in L} p_l)$  is bounded by  $e_{q_r, r}$ , and  $e_{q_r, r}$  depends only on the type of error location and  $q_r$ . (The notation “( $A$ )” appended to “independent” modifies the meaning of independent.) Here, products such as  $\prod_{k \in K} q_k$  informally denote the combination of error events where  $q_k$  occurs at its location  $k$ . If in this definition,  $L$  is restricted to subsets of  $K$ , and  $\pi$  is the identity map, then the model is independent( $B$ ). In particular,  $\text{Prob} \prod_{k \in K} q_k / \text{Prob}(\mathbb{1})$  is at most  $\prod_{k \in K} e_{q_k, k}$ , where  $\text{Prob}(\mathbb{1})$  is the probability of no error at any of the error locations. An error model satisfying only this last property is independent( $C$ ) or *quasi-independent* [8]. The heuristic analysis reestablishes full independence at each stage and can be considered as an attempt to capture and maintain independence( $A$ ).

In the three error models of the previous paragraph, the  $e_{p,l}$  are ratios of error probabilities, so they are called *error likelihoods* for the remainder of this paper. If the errors are independent for different locations and the error parameters are chosen optimally, then the (marginal) probability of  $p \neq \mathbb{1}$  acting at  $l$  is given by  $e_{p,l} / (1 + \sum_{q \neq \mathbb{1}} e_{q,l})$ . In particular, the error likelihood is larger than the marginal error probability. The error likelihoods  $e_{q,l}$  are assumed to depend only on the type of gate with which the error location  $l$  is associated. The analysis is implemented so that any such gate-dependent combination of  $e_{q,l}$  can be used as the physical error model. For the examples given, a uniform-error model is used for physical gates. The computationally determined logical-gate error models deviate significantly from the uniform-error model. For the primary scheme, only cnot, preparation and measurement errors play a role. These are parameterized by likelihoods  $e_c$ ,  $e_p$  and  $e_m$ . For a cnot’s error location, there are 15 possible non-identity Pauli products, each of which has likelihood  $e_c/15$ . The total probability of error is  $e_c/(1 + e_c)$ . For preparation and measurement of  $X$  and  $Z$  eigenstates, only one type of Pauli-operator error needs to be considered ( $Z$  and  $X$  errors, respectively). For universal quantum computation, the Hadamard gate and additional state preparations are needed. For a Hadamard gate, each of the three non-identity Pauli operators has likelihood  $e_h/3$ . The additional state-preparations’ errors can also be described as applications of one Pauli operator. The error for preparation of  $|i\pi/4\rangle$  ( $|\pi/8\rangle$ , respectively) is taken to be random- $Z$  ( $Y$ , respectively) error with a likelihood of  $e_s$ . To reduce the parameter space, set  $e_s = e_p = e_m$  and  $e_h/(1 + e_h) = 3e_p/(2(1 + e_p))$ . This is consistent with the assumption that errors of one-qubit gates are depolarizing and independent of the gate.

Since the analysis assumes probabilistic errors, it does not directly address the question of what happens when there are coherences between different error combinations expressed as Pauli products. Such coherences cannot be ignored. For example, decay of  $|1\rangle$  to  $|0\rangle$  cannot be expressed as a probabilistic Pauli-operator error. In this case, the likelihoods have to be replaced by (relative) amplitudes. In principle, error amplitudes can be formalized by means of environment-labeled error sums, see [8, 23]. Previous threshold analyses that take this into account suggest that results obtained for probabilistic errors extend to independent( $C$ ) non-probabilistic errors, but it may be necessary to square the maximum tolerable errors in the worst case, see [24, 25]. For example, if 0.01 probability of error is acceptable in the probabilistic model, then in the coherent model, this may have to be reduced to 0.0001. However, this conclusion seems overly pessimistic. First, error control based on stabilizer techniques is designed to remove coherences between differently acting combinations of Pauli-product errors as fast as possible, so there should be little opportunity for

coherences to add as amplitudes rather than as probabilities. Second, at the cost of increasing the error per operation, it is possible to deliberately randomize the computation by applying canceling random Pauli products before and after Hadamard and cnot gates. Random stabilizing Pauli operators may be applied after state preparations and before measurements. This ensures that interference between error amplitudes is well suppressed even before error detection or correction is used. This is a version of the twirling method used in entanglement purification [26]. Finally, it is interesting to note that one of the error-detecting codes used here is the same as the amplitude damping code given on page 99 of Gottesman’s thesis [27].

Another type of error not considered by the probabilistic model is leakage and qubit-loss error, whereby amplitude is lost from a qubit to an orthogonal state space. Fortunately, the teleportation based methods solve this problem implicitly by constantly refreshing the qubits used. The effect of leakage on the Bell state measurements is no different from other measurement errors. For leakage due to qubit-loss, there is in addition the opportunity to detect the error, which can be taken advantage of in error-correction [2].

### III. ANALYSIS OUTLINE

Because the basic codes are CSS codes, encoding and decoding operations require only cnots,  $X$ - and  $Z$ -postselected measurements, and preparation of the  $+1$  eigenstates of  $X$  ( $|+\rangle$ ) and  $Z$  ( $|0\rangle$ ). Therefore, the first task of the scheme is to use concatenation to implement these operations with arbitrarily low error after postselection. Errors are controlled by purifying prepared states at each level and by using teleported error-detection in conjunction with each operation implemented. At all times, the total state is a CSS state, and error behavior can be tracked by computing the likelihoods of each possible syndrome. Subroutines that compute likelihoods either formally or with high-precision arithmetic were implemented using a standard computer algebra language and are described in Sect. V. Because there are exponentially many syndromes, it is unfeasible to track them explicitly except for small numbers of qubits at a time. To analyze the scheme, the error behavior at each level is abstracted by modeling it in terms of a *logical-error model* associated with encoded gates applied at the current top level, and a *terminal-error model* of errors acting on encoded qubits at each level after the logical errors. The heuristic involves using independent errors for the two models. The error likelihoods are chosen with the intention of bounding the true error likelihoods from above after normalizing the likelihood of having no error anywhere to 1. The error models are described in Sect. IV. The logical- and terminal-error models are constructed level by level. The main step of this construction is to explicitly compute the error behavior of the purified encoded Bell pair needed to implement gates at the next level. Because the Bell pair involves only two blocks of 4 qubits and a purification step uses two such pairs at a time (involving a total of 16 qubits), this can be done to arbitrary precision with reasonable computational resources. The original scheme suggested using one purification cycle consisting of two purification steps to prepare a “good” encoded Bell pair. Although this reduces probabilities of undesirable syndromes (those involving an undetectable encoded error) to second order, it is insufficient for good independence properties. For the purpose of analysis, this is remedied by a second purification cycle. At this point, the true error in the encoded Bell pair has the same order behavior as independent error applied to each qubit. The heuristic replaces the true error model by a block-wise independent *Bell-error model*. The likelihoods for the Bell-error model are computed so as to approximate relative likelihoods of the computed model without any obvious biases that may reduce predicted error probabilities. The procedure is discussed in Sect. VI. Block-wise independence is needed to ensure that each logical gate’s error is independent and independent of the terminal-error model.

With this assumption, the teleported implementation of gates ensures that different steps of a logical computation are isolated. The independence of the Bell error model also makes it possible to directly compute logical-error likelihoods for state preparation and measurement (Sect. VII). Similarly, the logical-error likelihoods for the cnot can be computed. However, because the cnot is implemented directly rather than by explicitly using lower-level encoded cnots, the computation depends on whether it is for the physical level or for higher levels. This is explained in Sect. IX. The main application of postselected fault-tolerant quantum computation is to the preparation of arbitrary stabilizer states in a fault-tolerant manner. To do so one first prepares the desired state in encoded form at the top level of the concatenated error-detecting codes. One then decodes the error-detecting codes, accepting the result only if no errors are detected. The error associated with decoding is, according to the heuristic, independent between logical qubits. How to compute it at each level of the concatenation hierarchy is discussed in Sect. XI. To complete the analysis, it is necessary to determine the error of encoded Hadamard gates and of encoding the two states needed for universal quantum computation. This is done in Sect. X and Sect. XII. The results for specific error models and the implications for scalable quantum computations are given in Sect. XIV. The results are discussed in Sect. XV.

#### IV. REPRESENTING THE ERROR BEHAVIOR

The scheme for postselected quantum computation is to be analyzed one level at a time. At a given level, an encoded postselected computation is implemented. Although the entire computation occurs in parallel, the analysis considers the computation sequentially from state preparation onward. Thus, it makes sense to talk about the current state  $|\psi\rangle$  of the logical computation.  $|\psi\rangle$  is a state of  $n$  logical qubits, each encoded with  $4^h$  physical qubits, where  $h$  is the current level of the concatenation hierarchy. (Level 0 is the physical level.)  $|\psi\rangle$  is modified from the ideal, error-free state  $|\psi_I\rangle$  by errors. The effect of these errors is separated into *logical errors*, which can be attributed to errors in the steps of the logical computation so far, and *terminal errors*, which act after the logical errors and directly on encoded qubits at each level. Most terminal errors are detectable and are eliminated in the next step of the computation.

Logical errors are modeled by independent errors acting at error locations associated with logical gates. Like the physical-error model, they are characterized by likelihoods of Pauli products for locations associated with each gate and depend only on the type of gate, not the specific instance. Logical errors on the current state of the computation affect solely the logical qubits. They can be detected only by implementing the next level's operations.

Terminal errors are modeled as errors acting after, and independently of, the logical errors. Consider the blocks of four physical qubits encoding first-level qubits. The terminal error model  $T_0$  consists of a fixed distribution of four-qubit Pauli products acting independently on each block. The distribution can be simplified using the stabilizer for each block. For example, if the spectator qubit is in the state  $|\mathfrak{o}\rangle_{\mathfrak{s}}$  (see [1]), then the stabilizer is generated by  $[XXXX]$ ,  $[ZZZZ]$  and  $[IIZZ]$ , and consists of 8 Pauli products. As a result, the  $2^8$  four-qubit Pauli products consist of  $32 = 2^5 = 2^{8-3}$  distinct cosets of the stabilizer, where each coset has the same effect on the block. Thus  $T_0$  is defined by associating a likelihood to each of the 31 non-identity cosets, normalizing the likelihood of the identity coset to 1. These likelihoods must be computed based on how the states of the blocks are obtained. In this case, each block originates from the destination block of an encoded Bell pair used in a teleportation step. The explicitly computed likelihoods of the encoded Bell state's errors are seen to satisfy some independence criteria between the two blocks. In fact, the computed likelihoods are not far from what would be obtained by acting on each



qubit independently. This ensures that using a block-wise independent error model to bound the likelihoods is at least reasonable. That the computed likelihoods are related to a qubit-independent error model can be used for choosing likelihoods for the 31 non-identity cosets. The likelihoods thus obtained form the Bell-error model. The part acting on the destination blocks determines the level-1 terminal-error model. For each level  $l \geq 2$ , further independent terminal errors are obtained by computing the error likelihoods for encoded Bell states prepared at this level by use of lower level gates. The errors of  $T_{l-1}$  act on level- $(l-1)$  qubits that form a block encoding level  $l$  qubits. The independent combination of the errors of  $T_l$  up to level  $h$  constitutes the terminal-error model for level  $h$ . If physical errors are sufficiently low for the scheme to scale, each contribution  $T_l$  to the terminal error model has the property that errors with significant likelihood change the syndrome for the code at level  $l$ , making them detectable in future steps. Errors that change the encoded qubit without affecting the syndrome are at least quadratically suppressed. Although the actual state of the computation is always extremely noisy due to the terminal error model, conditional on the syndrome of the concatenated error-detecting code being  $\mathbf{0}$ , the state is reliable. When using the state in a destructive measurement or by decoding the error-detecting code, the relevant parts of the syndrome are verified so that postselection eliminates the non- $\mathbf{0}$  syndrome events to the extent that it is necessary to do so.

## V. COMPUTATIONAL METHODS

There are two principal tasks that require computer assistance. The first is to determine the error likelihoods of syndromes for stabilizer states given a network to prepare them and given the error likelihoods associated with gates and other states used by the network. The second is to approximate the error likelihoods computed for the purified encoded Bell pairs by block-wise independent likelihoods. Functions to perform these tasks were implemented using a standard computer-algebra system. The functions are included with the electronic files submitted to `quant-ph` (available at <http://arxiv.org/>) and are also available by request from the author. For the first task, a stabilizer state with error is represented by an array of error likelihoods with one entry for each syndrome value. The stabilizer state is specified by the generator matrix  $Q$  for the stabilizer as defined in [2]. The syndrome is a 0 – 1 vector characterizing the eigenvalues of the Pauli product operators represented by the rows of  $Q$ . For a stabilizer state on  $n$  qubits, the generator matrix is  $n \times 2n$  and the syndrome is an  $n$ -vector. Thus, a stabilizer state with error is specified by the pair  $Q$  and an array of  $2^n$  likelihoods, one for each of the  $2^n$  possible values of the syndrome. The probabilities can be derived from the likelihoods by dividing by the sum of the  $2^n$  likelihood values. For flexibility, the functions were implemented so that the likelihoods could be computed as polynomials of a single error parameter. Typically, higher degree terms of these polynomials contribute very little, and to take advantage of this, the computations estimate the highest-degree term by making use of an upper bound on the value of the error parameter. These formal computations were used to verify that undetected errors are indeed suppressed to second order. However, for determining whether a given error rate is below the threshold, high precision arithmetic was used.

To compute syndrome likelihoods for states produced by small networks, the following four functions are needed:

1. Adding a new qubit in the state  $|0\rangle$  or  $|+\rangle$ . This involves expanding the generator matrix, adding a new row, and expanding the likelihood array by a factor of two.
2. Applying error-free cnots and Hadamard gates. This is a transformation of the generator matrix that requires multiplication on the right by the appropriate linear transformation. The

syndrome array is not affected.

3. Applying errors according to an error model. Error models include those corresponding to applying Pauli products to an error location involving one or two qubits according to a likelihood distribution. This was implemented by subroutines that compute the effect of Pauli products on syndromes (the generator matrix is unchanged) and that are able to convolve the error model's likelihoods with the syndrome likelihoods.

4. Projecting a qubit's state onto the  $|0\rangle$  or  $|+\rangle$  states. This is the step involving postselection. It requires a row transformation of the generator matrix with an associated transformation of the syndrome array to ensure that only the last row (if any, case 1) involves an operator not commuting with the qubit projection. If there are no such rows (case 2), then the row transformation is such that the first  $n - 1$  rows involve the identity operator acting on the projected qubit. In case 2, the transformation is arranged so that the last row's operator acts only on the projected qubit. The syndrome array is then reduced. In case 1, the new syndrome likelihoods are obtained as sums of the two likelihoods associated with the two possible eigenvalues of the operator represented by the last row. In case 2, the new syndrome likelihoods are given by the likelihoods associated with eigenvalue  $+1$  of the operator represented by the last row. After the new syndrome array has been obtained, the two columns corresponding to the projected qubit and the last row are deleted from the generator matrix.

In addition to the four functions above, several auxiliary functions were implemented. For example, it is convenient to be able to apply any desired row transformation to the generator matrix, which also permutes the syndrome array. The mathematical details needed to implement all these functions are given in [2].

It is useful to observe that the likelihoods are always positive and that all the operations used involve only addition and multiplication of positive numbers. This ensures that numerical errors do not spread too rapidly. The computer algebra system used has the capability to keep track of the precision of likelihoods and likelihood ratios obtained. That the results have sufficient precision was verified by inspecting the recorded precision provided by the computer-algebra system.

The method for obtaining the Bell-error model from the computed likelihood distribution for the purified encoded Bell pair is described in the next section.

## VI. PREPARATION OF THE ENCODED BELL PAIR

The original scheme for postselected quantum computation is based on concatenation of two four-qubit error-detecting codes that are used alternately at different steps of the computation. Each step of the computation is based on teleportation through a Bell pair encoded in the two codes. This state is purified once before being used. For the purpose of the computer-assisted analysis used here, the scheme is modified in two ways. First, only one four-qubit code is used within a level, necessitating a change in the preparation of the encoded Bell state. See Fig. 1. Second, a single purification does not result in sufficient independence between the two codes supporting the Bell pair, so two purification steps are used. This results in independence to lowest order. It is expected that it is not necessary to implement this in practice. Ideally, the purification method used asymptotically leads to block-wise independent error behavior. Unfortunately, this is not the case for the purification scheme used here, which is based on the standard entanglement purification protocol [28]. An alternative approach to purification is to use the methods of Shor [3] and generalized by Steane [29] to purify the encoded Bell state by measuring syndromes with specially prepared "cat" states. Although this still does not lead to asymptotic independence, it may reduce the resources required while still approaching independence sufficiently well for

practical purposes.

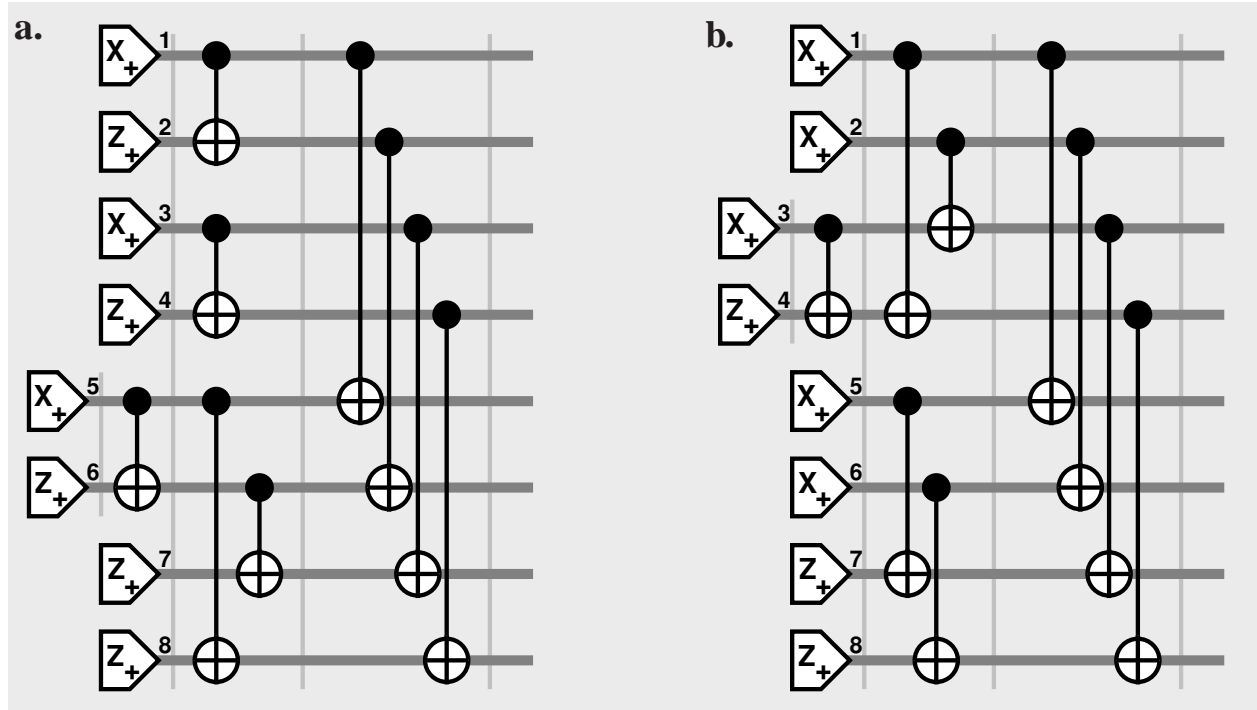


FIG. 1: States used to teleport encoded qubits. The conventions for network elements are as in [1] At each level a choice is made whether to have the spectator qubit in its  $|0\rangle_S$  or its  $|+\rangle_S$  state. Network **a.** makes the encoded Bell state with both spectator qubits in state  $|0\rangle_S$ . The output of network **b.** has both in state  $|+\rangle_S$ . The stabilizer of **a.**'s output is

$$\begin{aligned} & [XXXXIIII], [ZZZZIIII], [IIZZIIII], \\ & [IIIXXXXX], [IIIZZZZZ], [IIIIIZZ], \\ & [XXIIXXII], [ZIZIZIZI]. \end{aligned}$$

The third and sixth Pauli product are the spectator qubits'  $Z$  operators. The logical qubits' operators are  $X^{(L_1)} = [XXIIIIII]$ ,  $Z^{(L_1)} = [ZIZIIIII]$ ,  $X^{(L_2)} = [IIIXXXII]$ ,  $Z^{(L_2)} = [IIIZIZI]$ . Thus the last two operators are stabilizers of the encoded Bell pair. Similarly, the stabilizer of **b.**'s output is

$$\begin{aligned} & [XXXXIIII], [ZZZZIIII], [IXIXIIII], \\ & [IIIXXXXX], [IIIZZZZZ], [IIIIIXIX], \\ & [XXIIXXII], [ZIZIZIZI], \end{aligned}$$

where the third and sixth Pauli product are the spectator qubits'  $X$  operators.



The first step of the analysis requires determining the syndrome likelihood distribution of the encoded Bell pair if the preparation method of Fig. 1 is used with two purification cycles. Each purification cycle involves two steps, purifying  $Z$ -type and  $X$ -type syndromes, respectively. The order of the two steps is randomized. At each level, a choice is made of whether to use spectators in  $|0\rangle_S$  or  $|+\rangle_S$  states. The choice must be made based on the error models for gates at the current level, as  $|0\rangle_S$  spectators help with suppressing  $X$  errors, whereas  $|+\rangle_S$  spectators suppress  $Z$  errors. In either case, the syndrome distribution of the prepared encoded Bell pairs is computed by using the functions that can simulate the preparation networks and apply each step's error model. The randomization of the purification order is implemented by computing likelihoods for both possible orders and averaging them. In order for this averaging to be correct, the normalization (sum of the likelihoods) must be identical in the two cases. This condition is satisfied because each case involves the same gates but in a different order. This procedure yields the *computed error model* for the encoded Bell pairs.

If the likelihood distribution is computed formally, with cnot preparation and measurement errors all being a multiple of a single error parameter  $e$ , inspection shows that the lowest-degree contribution to the likelihood of a syndrome is the same as the minimum weight of the set of Pauli products that can give rise to that syndrome. In other words, the likelihood distribution has error behavior of the same order as that obtained if independent errors are applied to each qubit after preparing the stabilizer state without errors. (This is not the case if only one purification cycle is used.) This motivates the next step, which is to heuristically bound the error-likelihood distribution with an independent-error model. Only independence between the origin and destination block of the encoded Bell pair is needed. The error model is therefore designed to independently apply certain Pauli products to each block of the encoded Bell pair. Consider the origin block. Because the stabilizer consists of products of the three operators  $[XXXX]$ ,  $[ZZZZ]$  and  $[IIZZ]$  or  $[IXIX]$  (depending on whether the spectator qubit's state is  $|0\rangle_S$  or  $|+\rangle_S$ ), and because two Pauli products differing by an element of the stabilizer have the same effect, the set of Pauli products can be partitioned into 32 cosets, where two operators in the same coset have the same effect on the encoded Bell pair. The independent-error model assigns a likelihood to each of these 32 cosets for the origin block, and similarly for the destination block. Because of the encoded stabilizer operators  $[XXIIXXII]$  and  $[ZIZIZIZI]$  characterizing the encoded Bell state, each syndrome of the encoded Bell pair can be obtained in four different ways from errors on the two blocks as classified by the 32 cosets. The problem is to choose the origin and destination Bell-error models to match the computed error model as closely as possible without unintentionally improving future error behavior. Thus, the goal is to have the Bell-error model's normalized likelihoods exceed the computed error model's normalized likelihoods. (The normalized likelihoods are such that the likelihood of the 0 syndrome is 1.) Although it cannot be excluded that increasing likelihoods in this way leads to sufficient error cancellation to improve the error behavior, this seems unlikely. A second goal is to recover the same error model if indeed it is induced by independent errors. The computational method used to obtain the independent Bell-error model is heuristic (see the next paragraph), but achieves these goals to good approximation. One way to measure the quality of the Bell-error model is to calculate the maximum and minimum ratios of the normalized likelihoods of corresponding syndromes in the Bell-error model and the computed error model for the encoded Bell state. Ideally, the minimum ratio should be 1. It was found to be greater than  $1 - 10^{-6}$  in all cases and usually much closer to 1. The maximum ratio varies significantly and is largest when the preparation/measurement error dominates. See Fig. 2.

To obtain the block-wise independent Bell-error model, each encoded Bell pair syndrome is assigned a weight. For unbiased errors, the weight should be the minimum weight of Pauli prod-

ucts that can give rise to the syndrome. Because errors in the models in effect at higher levels of concatenation are highly biased, the weight computation is modified as follows. First a one-qubit error model is derived from the maximum marginal error probabilities of the likelihoods for Pauli products after the cnot. After normalizing the identity error to 1, the negative logarithm of the error likelihoods of  $X$ ,  $Y$  and  $Z$  are assigned as weights to each of these Pauli operators. The weight of a Pauli product is the sum of the weights of each one-qubit factor. Each syndrome's weight is given by the minimum weight of Pauli products that give rise to it. Similarly, the weights of the 32 cosets for the origin and destination blocks are computed and each coset  $c$  is assigned to the minimum weight Pauli product  $p(c)$  that belongs to the coset. Next, each computed error likelihood associated with a non-zero syndrome  $s$  for the encoded Bell pair is attributed to one of the four pairs of origin and destination block cosets that can give rise to  $s$ . The choice is made so as to minimize the sum of the weights of the two cosets. As a result, each pair of cosets  $c_1, c_2$  is assigned an error likelihood  $e(c_1, c_2)$ , which is 0 if it does not have minimum weight for the encoded Bell-pair syndrome that is determined by the pair. Let  $s(c_1, c_2)$  be the encoded Bell-pair syndrome determined by  $(c_1, c_2)$ . The last step is to obtain independent origin and destination likelihoods  $e_o(c)$  and  $e_d(c)$  that, in a sense, bound the likelihoods obtained for the pairs. This is done by minimizing the independent likelihoods of each block subject to the constraint that if  $(c_1, c_2)$  is a pair of cosets and the weight of  $s(0, c_2)$  is less than the weight of  $s(c_1, c_2)$ , then  $e_o(c_1)/e(0) \geq e(c_1, c_2)/e(0, c_2)$ , and similarly if the weight of  $s(c_1, 0)$  is less than the weight of  $s(c_1, c_2)$ . The idea is for the independent-error model to have larger relative likelihoods consistent with independence( $B$ ).

The Bell-error model need not have the same error behavior for the origin and destination blocks. However, the two blocks can be made to behave similarly by symmetrizing the preparation procedure. This is done by randomizing the orientation of the Bell pair, which is made possible by using the same spectator qubit state on each block.

In the next sections, the independence of the Bell error model is used both to simplify the computation of the next level's encoded gates and to ensure that the desired independence properties apply throughout a computation. Numerical results are presented in Sect. XIII.

## VII. STATE PREPARATION

Preparation of encoded states is implemented by postselected measurements of the origin block of an encoded Bell pair. For preparing the logical  $|0\rangle_L$  ( $|+\rangle_L$ ) state,  $Z$  ( $X$ ) measurements on each origin qubit postselected on the  $+1$  eigenvalue are used. The resulting state on the destination qubits must be modeled by an independent preparation error acting on the logical qubit, followed by the terminal-error model derived from the destination block's Bell-error model. With the independence heuristic, the effect of the measurement of the origin block's qubits depends only on the errors acting on the origin and propagates into the encoded qubit via the encoded entanglement. To compute the propagated error, observe that because the origin errors are now assumed to be independent of the destination errors, it is possible to abstract the destination before the destination errors are applied as a single, error-free qubit  $B$  entangled with the origin's encoded qubit. The effect of measurement can then be computed explicitly using the functions of Sect. V. The measurement results in either the desired state on  $B$  or the orthogonal state. The probability that the orthogonal state is obtained defines the independent contribution to the logical error due to state preparation.

## VIII. MEASUREMENT

Postselected measurement is similar to state preparation. It involves making the same measurements, but on the destination block of an encoded Bell pair. As a result, the analysis can be done in the same way, which is by modeling the origin half as an ideal single qubit entangled with the logical qubit of the destination. The effect of measurement can be computed explicitly to determine the likelihoods for the state that the single qubit ends up in. Note that in an implementation it may be the case that the origin half has already been involved in a postselected Bell measurement. The effect of such prior operations is taken into account by independent logical errors active in the current state. These errors are independent of the destination errors, making it possible to model the effects of measurement as has been done here. The randomized symmetrization of the Bell pair result in logical errors for measurements that are essentially the same as the logical errors for preparation.

## IX. CNOT

The encoded cnot is implemented transversally by applying cnots to corresponding qubits in the two blocks encoding the qubit to be acted on. This is followed by a teleportation step that involves postselected Bell measurements from the encoded qubits' blocks to the origin blocks of two encoded Bell pairs. To avoid delays, the cnots of the Bell measurements can be interleaved with the transversal cnots [1]. The independence heuristic implies that logical errors attributable to the transversal cnots and Bell measurements are independent of earlier logical errors, terminal errors of qubits not involved in the gate, and destination Bell errors for the two Bell pairs used for teleportation. As a result, the effect of the encoded cnot can be computed by using only four blocks whose errors are characterized by the independent destination and origin Bell-error models. As was done for measurement and preparation errors, each of these four blocks' encoded qubit is considered entangled with an ideal reference qubit. In this way, the complete error behavior of the cnot implementation can be computed.

If the qubits of the blocks are themselves encoded with the error-detecting codes of the scheme, the cnot analysis is modified. This is necessary because rather than implementing each cnot according to the lower-level instructions, the cnots are implemented as transversal physical cnots, acting on corresponding physical qubits. This improves the error behavior of the encoded cnot because the effect at higher levels is that the implementation of the cnot behaves as if the Bell measurement were error-free. To see this, consider the logical-error model for the cnot derived at level 1. It is possible to virtually rearrange the cnots and errors of the cnots and measurements so that (a) the transversal cnot is applied first without errors, (b) all the errors occur (including those due to origin and destination error models), and finally, (c) the Bell measurements are implemented without errors. The computed logical error of the procedure is determined by those error combinations in this virtual representation that satisfy the condition that corresponding origin and destination syndromes are identical. Consider the next level of encoding. The cnot implementation consists of applying the lower-level scheme to corresponding physical origin and destination blocks. The computed error for these cnots anticipates the Bell-measurement errors so that it is not necessary to re-introduce them. That is, in computing the next-level cnot's logical-error likelihoods, the transversal cnots come with the previously computed logical errors, but the Bell measurements can be taken to be error-free.

## X. HADAMARD GATE

The Hadamard gate is not needed for scalable postselected generation of CSS states. However, it is helpful for achieving universality. The computation of its contributions to the logical error is similar to that of the cnot. A teleported implementation may be used where the Hadamard is applied transversally to the current block of a logical qubit, followed by a Bell measurement involving an origin block of an encoded Bell pair. The code requires that the middle two qubits be swapped after the transversal Hadamard, which can be taken into account by “crossing” the middle two Bell measurements. Again, at levels other than the first, the Hadamard is implemented in a transversal fashion rather than reimplemented using explicit lower-level gates. As a result, the computation of higher-level logical errors can be simplified by having error-free Bell measurements.

## XI. DECODING A PREPARED STATE

The main application of postselected fault-tolerant quantum computation is to the preparation of stabilizer states with errors that are primarily local. These states can then be used in a standard fault-tolerant quantum computation. They are prepared first in encoded form at a sufficiently high level of encoding using the error-detecting codes. Once such a state is obtained, the error-detecting codes are decoded from the bottom up. The heuristic error model used to describe the error behavior of the scheme implies that any encoded stabilizer state obtained before decoding the error-detecting code is subject to logical errors due to the gates used to prepare the encoded state, and terminal-errors that are independently applied to each block at every level. The bottom-up decoding process adds errors to the final state only through undetected terminal errors and errors introduced in the decoding process itself. Because of independence, the error introduced in this way in the first step of the bottom-up decoding process can be computed from the terminal error model that applies to physical blocks. This error propagates as an additional local error in the next-level blocks. Since the terminal-error models at each level are themselves independent, this local error can be added independently to the next level’s terminal error model. The effect of the next level of decoding can then be computed as before. Thus, in each decoding cycle, additional local error from below is merged with terminal errors and decoding errors, conditioned on a successful decoding. Scalability is verified by confirming that the error pushed into the decoded qubit is bounded. A bound can be estimated by implementing this procedure for the first few levels to compute the decoding error in each step. In the examples computed (see Tables 1, 2), the local error introduced by decoding at each level appears to slowly decrease toward a steady state.

## XII. ENCODING AN ARBITRARY STATE

To encode an arbitrary state, a Bell pair is encoded at the top level of the concatenation hierarchy. The origin block of the pair is decoded bottom-up as in the process for preparing a stabilizer state in the previous section. The last step is to teleport a state prepared in a physical qubit into the top-level code using the decoded origin qubit. This process may be referred to as *injecting* a state into a code. The new state’s error model fits the logical/terminal error model scheme used before, where the terminal error is due to the terminal-error model applicable to the destination block of the encoded Bell pair. The logical error comes from the bottom-up decoding, the (post-selected) Bell measurement used for teleportation, and any error in the physical qubit’s state. Given the

bound on the bottom-up decoding error, it suffices to combine it with a bound on the error in preparing the desired state in a physical qubit and the error due to a physical Bell measurement.

### XIII. POSTSELECTED THRESHOLD

By use of the computer-assisted heuristics described in the previous sections, it is now possible to determine whether a given physical-error model is scalable for postselected computation with the error-detecting schemes under analysis. A physical-error model is scalable for preparing CSS states if the logical error probabilities can be made arbitrarily small. Universality requires logical state preparations and purifications. Consider preparation of logical  $|\pi/8\rangle$  states. A version of the purification scheme for  $|\pi/8\rangle$  states given in [1] is analyzed by Bravyi and Kitaev [30] in the context of “magic states distillation”. They show that magic states, which include  $|\pi/8\rangle$ , are distillable given a way of preparing them with probability of error below about 35 %, assuming no error in Clifford group operations. Encoding  $|\pi/8\rangle$  by decoding one-half of a logical Bell pair and teleporting introduces relatively little additional error (see below). These observations apply also to  $|i\pi/4\rangle$  preparation. As a result, error in preparation of logical  $|\pi/8\rangle$  and  $|i\pi/4\rangle$  states is not a bottleneck for scalability.

To illustrate the computer-assisted heuristic analysis, the logical error probabilities are graphed for a range of preparation/measurement and cnot errors in Fig. 2, which maps the maximum of the logical-error probabilities for encoded preparation, measurement, cnot, and Hadamard gates as a function of the physical-error probabilities and the number of levels of encoding. As can be seen, a small number of levels suffice to strongly suppress the logical-error probabilities. A boundary between the region where errors are scalable and where they are unscalable (by these schemes) emerges as the number of levels are increased. For measurement/preparation error probabilities well below the cnot error probability, the boundary is between 3.5 % and 5 %.



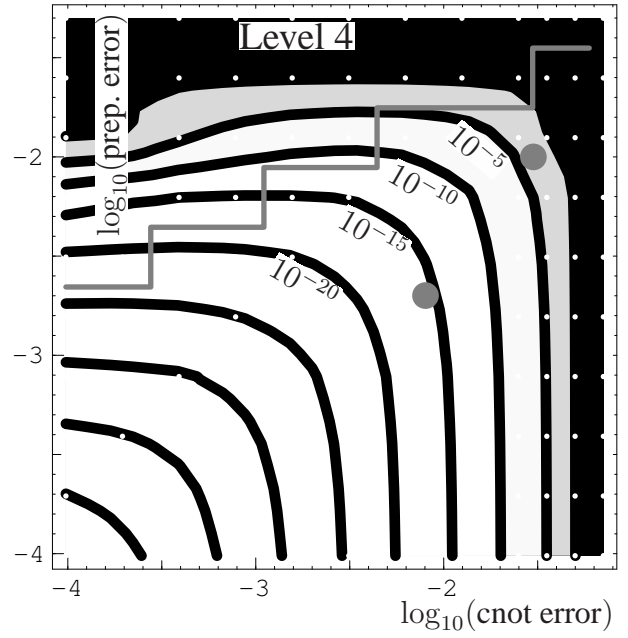
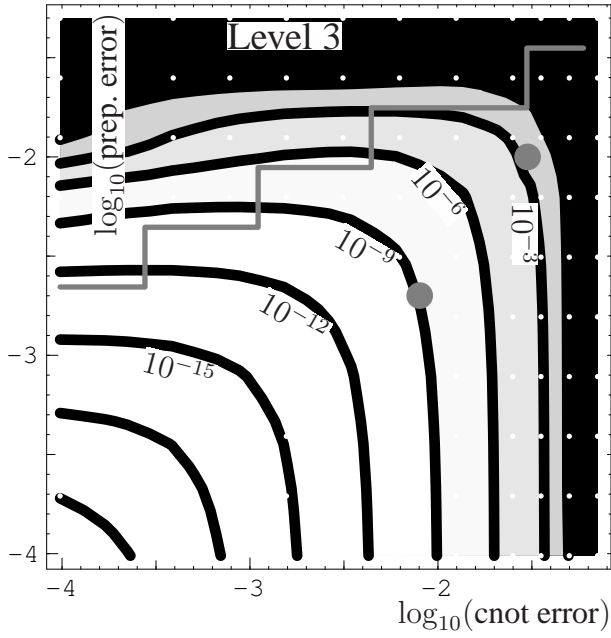
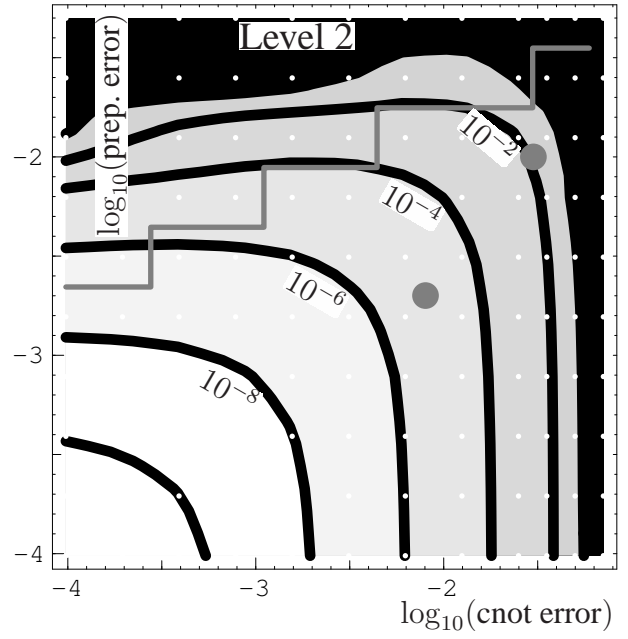
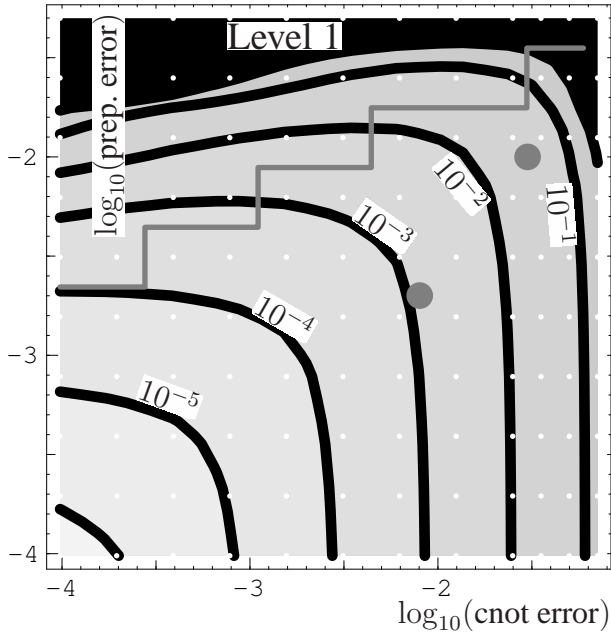


FIG. 2: Plots of error probabilities achieved after one, two, three and four levels of concatenation. The spectator qubits for the first level are in state  $|+\rangle_S$ . For the next three levels they are in state  $|0\rangle_S$ . The  $x$ - and  $y$ -axes show the  $\log_{10}$  of the total error probabilities of the physical cnot and the physical preparation/measurement, respectively. The Hadamard gate's error probability is  $3/2$  times the preparation/measurement error probability, consistent with the assumption that preparation and measurement error is comparable to other one-qubit gate errors except that one of the Pauli operators has no effect. The probability of each non-identity Pauli product contributing to the error is assumed to be identical. The contours show the maximum error probability of the encoded cnot, Hadamard and preparation/measurement gates at logarithmic intervals. The highest contour corresponds to a maximum error probability of  $.25$ . The contour intervals are adjusted from level to level. Darker shadings correspond to higher error probabilities. Black indicates the region where scalability clearly fails due to the error probabilities having exceeded  $.25$ . The contours were obtained by computing the error probabilities at 100 points in a  $10 \times 10$  logarithmic grid. The separation between adjacent grid points corresponds to a change in error probabilities by a factor of 2. An additional 20 points were computed for logarithmic cnot error probabilities of  $\log_{10}(0.071) = -1.15$ . and  $\log_{10}(0.0354) = -1.45$ . The positions of the points at which the probabilities were computed are shown as white dots. Interpolation was used to derive the contours. Note that the grid point separation corresponds to logarithmic intervals of about 0.3 (0.15 near the right scalability boundary). The contour positions, particularly the one at the scalability boundary, should therefore be regarded as having positional uncertainties of that order. The contours indicate decreasing error with increasing cnot error probabilities at high, constant measurement/preparation error rates. This is an artifact of the method used for obtaining the independent Bell-error error model. In particular, the quality of approximation of the independent-error model is not very good when preparation/measurement error is high compared to cnot error. This is probably because the method is based on cnot error and does not take preparation/measurement error into account. When the approximation is bad, the computed logical errors grow. The region where the maximum normalized likelihood ratio between the independent Bell-error model and the computed error model (see Sect. VI) exceeds 100 is above the gray staircase line in each plot. To determine the behavior of specific examples more precisely requires further computation. Two examples are given in Tables 1 and 2. The locations of the error probabilities used in the examples are indicated by the two gray points.

Two example error combinations are examined in detail in Tables 1 and 2. The first is near the scalability boundary for the scheme analyzed here. The second is lower by about a factor of 5. The measurement/preparation error probability is taken to be a factor of 3-4 below the cnot error probability. This choice is motivated by an estimate of how well measurement error can be suppressed by using ancillas and cnots [31]. As in Fig. 2, the Hadamard-gate error probability is  $3/2$  of the measurement/preparation error. The first example has all gate-error probabilities above 1 %. Specifically, the measurement/preparation error is 1 % and the cnot error is 3 %. Four levels are required to reach logical gate-error probabilities near or below  $10^{-4}$ . One more level reduces them below  $10^{-7}$ . The choice of spectator qubit state at each level significantly affects the logical gate error distributions. Note that  $Y$  errors are always significantly suppressed, which is a feature of CSS codes. Also, having the spectator qubit be in state  $|\phi\rangle_S$  strongly suppresses  $X$  errors compared to  $Z$  errors, except for the Hadamard gate. This is because the implementation of the Hadamard gate voids the ability of the teleportation step to detect errors affecting only the part of the syndrome due to the spectator qubits' states. The biases suggest that it may be worth using different codes adapted to this bias at the higher levels. The decoding error is clearly stable as more levels are added. In fact, it is monotone decreasing. By extrapolation, the total decoding error is below 2.3 % no matter how many levels are used. This implies that if a  $|\pi/8\rangle$  state is injected into the top level as discussed above, the newly encoded  $|\pi/8\rangle$  state should have error probability of at most 9 %, bounding the sum of the measurement/preparation error (1 %), the decoding error (2.3 %), and the Bell measurement error (5 %, due to the cnot and two measurements). This is well below the purification threshold [30].

The second example involves measurement/preparation error of 0.2 % and cnot error of 0.8 %, and exhibits similar features except that only two levels are needed to suppress the maximum error probability below  $10^{-5}$ . The decoding error probability decreases to a value below 0.55 %.

Error probabilities:	$e_p = e_m = 0.01, e_c = 0.03$			
Level 1	Spectator: $ +\rangle_{\xi}$			
Independence quality	3.20			
Prep./Meas. error	$X : 4.14 * 10^{-3}$	$Z : 9.82 * 10^{-4}$		Max: $4.14 * 10^{-3}$
Cnot marginal error	$X : 1.83 * 10^{-2}$	$Z : 6.11 * 10^{-3}$	$Y : 3.70 * 10^{-4}$	Total: $2.98 * 10^{-2}$
Hadamard error	$X : 1.10 * 10^{-2}$	$Z : 1.10 * 10^{-2}$	$Y : 2.31 * 10^{-3}$	Total: $2.44 * 10^{-2}$
Decode error	$X : 5.61 * 10^{-3}$	$Z : 1.30 * 10^{-2}$	$Y : 4.75 * 10^{-3}$	Total: $2.34 * 10^{-2}$
Level 2	Spectator: $ o\rangle_{\xi}$			
Independence quality	8.59			
Prep./Meas. error	$X : 4.87 * 10^{-4}$	$Z : 4.34 * 10^{-4}$		Max: $4.87 * 10^{-4}$
Cnot marginal error	$X : 5.03 * 10^{-3}$	$Z : 3.39 * 10^{-3}$	$Y : 8.33 * 10^{-6}$	Total: $9.53 * 10^{-3}$
Hadamard error	$X : 6.02 * 10^{-3}$	$Z : 6.02 * 10^{-3}$	$Y : 1.24 * 10^{-4}$	Total: $1.22 * 10^{-2}$
Decode error	$X : 1.30 * 10^{-2}$	$Z : 4.86 * 10^{-3}$	$Y : 4.56 * 10^{-3}$	Total: $2.24 * 10^{-2}$
Level 3	Spectator: $ o\rangle_{\xi}$			
Independence quality	2.64			
Prep./Meas. error	$X : 5.10 * 10^{-6}$	$Z : 2.42 * 10^{-4}$		Max: $2.42 * 10^{-4}$
Cnot marginal error	$X : 9.37 * 10^{-5}$	$Z : 1.22 * 10^{-3}$	$Y : 4.19 * 10^{-8}$	Total: $1.57 * 10^{-3}$
Hadamard error	$X : 7.27 * 10^{-4}$	$Z : 7.27 * 10^{-4}$	$Y : 7.39 * 10^{-7}$	Total: $1.45 * 10^{-3}$
Decode error	$X : 1.23 * 10^{-2}$	$Z : 4.55 * 10^{-3}$	$Y : 4.34 * 10^{-3}$	Total: $2.12 * 10^{-2}$
Level 4	Spectator: $ o\rangle_{\xi}$			
Independence quality	1.90			
Prep./Meas. error	$X : 3.11 * 10^{-10}$	$Z : 2.70 * 10^{-5}$		Max: $2.70 * 10^{-5}$
Cnot marginal error	$X : 2.08 * 10^{-8}$	$Z : 1.32 * 10^{-4}$	$Y : 1.07 * 10^{-12}$	Total: $1.59 * 10^{-4}$
Hadamard error	$X : 3.60 * 10^{-5}$	$Z : 3.60 * 10^{-5}$	$Y : 1.31 * 10^{-9}$	Total: $7.19 * 10^{-5}$
Decode error	$X : 1.22 * 10^{-2}$	$Z : 4.24 * 10^{-3}$	$Y : 4.22 * 10^{-3}$	Total: $2.07 * 10^{-2}$
Level 5	Spectator: $ +\rangle_{\xi}$			
Independence quality	1.94			
Prep./Meas. error	$X : 3.65 * 10^{-15}$	$Z : 7.37 * 10^{-9}$		Max: $7.37 * 10^{-9}$
Cnot marginal error	$X : 2.35 * 10^{-14}$	$Z : 6.12 * 10^{-8}$	$Y : 3.74 * 10^{-22}$	Total: $6.87 * 10^{-8}$
Hadamard error	$X : 1.76 * 10^{-8}$	$Z : 1.76 * 10^{-8}$	$Y : 3.10 * 10^{-16}$	Total: $3.51 * 10^{-8}$
Decode error	$X : 4.16 * 10^{-3}$	$Z : 1.22 * 10^{-2}$	$Y : 4.16 * 10^{-3}$	Total: $2.05 * 10^{-2}$

TABLE 1: Details for physical error probabilities of 1 % for state preparation and measurement and 3 % for cnot. The independence quality is the maximum ratio of the normalized likelihoods of the independent Bell and the computed error models (see Sect. VI). The minimum ratio found was 0.99999957. Errors are given in probabilities. Preparation and measurement errors are identical, due to randomization of the encoded Bell pair preparation to ensure bilateral symmetry of the errors. For preparation and measurement, the probabilities are assigned to only one operator that affects the state or measurement result. For example, a  $|o\rangle$  preparation is affected only by  $X$  errors. The cnot errors shown are the maximum marginal probabilities for the given Pauli operators. The total error probabilities are computed by summing the probabilities of each Pauli error. The number of physical qubits per logical qubits at level 5 is 1024.

Error probabilities:	$e_p = e_m = 0.002, e_c = 0.008$			
Level 1	Spectator: $ +\rangle_{\mathcal{S}}$			
Independence quality	1.11			
Prep./Meas. error	$X : 1.71 * 10^{-4}$	$Z : 3.61 * 10^{-5}$		Max: $1.71 * 10^{-4}$
Cnot marginal error	$X : 8.09 * 10^{-4}$	$Z : 2.35 * 10^{-4}$	$Y : 2.76 * 10^{-6}$	Total: $1.27 * 10^{-3}$
Hadamard error	$X : 4.46 * 10^{-4}$	$Z : 4.47 * 10^{-4}$	$Y : 6.62 * 10^{-5}$	Total: $9.59 * 10^{-4}$
Decode error	$X : 1.15 * 10^{-3}$	$Z : 3.26 * 10^{-3}$	$Y : 1.11 * 10^{-3}$	Total: $5.52 * 10^{-3}$
Level 2	Spectator: $ o\rangle_{\mathcal{S}}$			
Independence quality	1.14			
Prep./Meas. error	$X : 2.58 * 10^{-7}$	$Z : 5.32 * 10^{-7}$		Max: $5.32 * 10^{-7}$
Cnot marginal error	$X : 2.56 * 10^{-6}$	$Z : 3.63 * 10^{-6}$	$Y : 1.85 * 10^{-11}$	Total: $7.01 * 10^{-6}$
Hadamard error	$X : 3.82 * 10^{-6}$	$Z : 3.82 * 10^{-6}$	$Y : 1.07 * 10^{-8}$	Total: $7.66 * 10^{-6}$
Decode error	$X : 3.21 * 10^{-3}$	$Z : 1.08 * 10^{-2}$	$Y : 1.08 * 10^{-3}$	Total: $5.38 * 10^{-3}$
Level 3	Spectator: $ o\rangle_{\mathcal{S}}$			
Independence quality	1.52			
Prep./Meas. error	$X : 5.95 * 10^{-13}$	$Z : 1.16 * 10^{-10}$		Max: $1.16 * 10^{-10}$
Cnot marginal error	$X : 1.86 * 10^{-11}$	$Z : 9.03 * 10^{-10}$	$Y : 9.29 * 10^{-21}$	Total: $1.04 * 10^{-9}$
Hadamard error	$X : 3.52 * 10^{-10}$	$Z : 3.52 * 10^{-10}$	$Y : 2.48 * 10^{-16}$	Total: $7.04 * 10^{-10}$
Decode error	$X : 3.21 * 10^{-3}$	$Z : 1.08 * 10^{-3}$	$Y : 1.08 * 10^{-3}$	Total: $5.37 * 10^{-3}$

TABLE 2: Details for physical error probabilities of 0.2 % for state preparation and measurement and 0.8 % for cnot. See Table 1 for a description of the entries. The number of physical qubits per logical qubit at level 3 is 64.

#### XIV. GENERAL THRESHOLD

A strategy for implementing a standard quantum computation is to use postselected quantum computation for preparing the encoded states needed for operations and error-correction based on a code  $C$  with good error-correction properties. Provided the logical errors ( $C$ -logical errors) for gates acting on states encoded with  $C$  are sufficiently small, standard schemes can be applied to  $C$ -encoded qubits to achieve scalability. These schemes are most efficient if the starting error rates (in this case the  $C$ -logical error rates) are already small. However, the cost of small  $C$ -logical errors can be a substantial increase in overhead for postselected state preparation. The tradeoffs involved are yet to be investigated. The states needed for computation with  $C$ -encoded qubits are encoded stabilizer states, encoded Bell pairs with cnot or Hadamard gates pre-applied, and encoded states such as  $|\pi/8\rangle$ . The latter may be noisy and purified later if desired. State preparation proceeds by first obtaining the desired state encoded at a suitable level of the concatenated error-detecting codes, then decoding the error-detecting code hierarchy. Three types of error affect the prepared state. The first is error associated with the encoded network used to prepare the state in encoded form. These errors are estimated by the logical error model at the top level of the error-detecting code hierarchy. The second is local error from decoding. It is, to a good approximation, independent from qubit to qubit and can be computed as shown in Tables 1, 2. The third is due to any memory errors arising from delays while waiting for the postselected measurements to complete.



The contribution of the first error type to  $C$ -logical errors can be estimated as the product of the number of logical gates used in the preparation of the needed states and the maximum error probability for top-level encoded gates. For scaling to work straightforwardly with  $C$ -encoded qubits and gates, the contribution of the first error type needs to be small compared to the effect on the logical qubits of local error due to decoding. This can be achieved by using sufficiently many levels of the error-detecting code.

To be specific, assume that the maximum  $C$ -logical error must be below  $10^{-4}$  for standard scalability schemes to apply and consider the first example, with memory/preparation error of 1 % and cnot error of 3 %. The decoding error is less than 2.3 % per qubit at any level after the second. Choose  $C$  such that given an error probability per qubit of 11 % or less, the probability that the error is not correctable is less than  $0.5 * 10^{-4}$ . Such codes exist. Let  $L$  be the length of an encoding network for pairs of encoded Bell pairs with a cnot pre-applied. Choose a level of encoding with the error-detecting code such that the top level logical error rate is much less than  $0.5 * 10^{-4} / L$  per gate. This implies that the intrinsically uncorrectable error per  $C$ -logical gate implemented by error-correcting teleportation is well below  $0.5 * 10^{-4}$ . It suffices to show that error that cannot be corrected due to excessive local errors arising from decoding the error-detecting code and other operations needed for the  $C$ -logical gate implementation is also below  $0.5 * 10^{-4}$ . Referring to [2], the scheme works if the total error probability from a Bell measurement, a possible memory delay and twice the 2.3 % decoding error is less than 11 %. The Bell measurement error can be estimated as 5 % (one cnot, two measurements). Therefore, if the contribution from memory error is less than about 0.4 %, the scheme is expected to be successful. However, the resources required for state preparation as outlined are daunting: at least five levels of concatenation of the error-detecting codes are required and the code  $C$  is likely to be complex. If the error rates of the second example apply, the number of levels of error-detecting codes and the required error-tolerance of  $C$  can both be significantly reduced. In general, a large reduction in overhead results from having lower physical error rates.

## XV. DISCUSSION

The evidence presented above suggests that it is possible to quantum compute with error rates above 1 % per gate. The next steps are to improve the efficiency of the scheme and to better determine the resources required as a function of error rates. Some aspects of the scheme as used in the analysis above are chosen for the purpose of simplifying the analysis. For example, the two purification steps in each encoded-Bell-state preparation can probably be replaced by one, or by a cat-state syndrome-extraction procedure as mentioned in Sect. VI. Further improvements can be obtained by adapting the code used to each level's error behavior. An important contribution to resource overheads is the probability of successful state preparations. This probability decreases rapidly with more levels of error-detecting code or with the complexity of the first level codes used for standard quantum computation. Without using special techniques, this probability decreases exponentially with the number of qubits involved. As a result, one should switch from a purely postselected scheme to one that permits recovery from error as soon as possible. One idea is to combine the advantages of both for state preparation at higher levels.

An interesting question is to consider the relationship between postselected and standard quantum computation in the presence of errors. Is it true that if postselected quantum computation is scalable for an error model, then so is standard quantum computation? Alternatively, it is possible that there are error models for which one can quantum compute arbitrarily accurately, but only with exponentially small probability of success. In the calculations shown here, scalability of CSS

gates seems to imply that universal quantum computation is scalable. Is this always the case?

### Acknowledgments

This work was supported by the U.S. National Security Agency. It is a contribution of the National Institute of Standards and Technology, an agency of the U.S. government, and is not subject to U.S. copyright.

- 
- [1] E. Knill (2004), quant-ph/0402171.
  - [2] E. Knill (2003), quant-ph/0312190.
  - [3] P. W. Shor, in *Proceedings of the 37th Symposium on the Foundations of Computer Science (FOCS)* (IEEE press, Los Alamitos, California, 1996), pp. 56–65.
  - [4] A. Y. Kitaev, in *Quantum Communication and Computing and Measurement*, edited by O. H. et al. (Plenum, New York, 1997).
  - [5] E. Knill and R. Laflamme, Tech. Rep. LAUR-96-2808, Los Alamos National Laboratory (1996), quant-ph/9608012.
  - [6] D. Aharonov and M. Ben-Or, in *Proceedings of the 29th Annual ACM Symposium on the Theory of Computation (STOC)* (ACM Press, New York, New York, 1996), pp. 176–188.
  - [7] D. Aharonov and M. Ben-Or (1999), quant-ph/9906129.
  - [8] E. Knill, R. Laflamme, and W. Zurek, Proc. R. Soc. Lond. A **454**, 365 (1998).
  - [9] D. Gottesman, Phys. Rev. A **57**, 127 (1998).
  - [10] E. Knill, R. Laflamme, and W. H. Zurek, Science **279**, 342 (1998).
  - [11] C. Zalka (1996), quant-ph/9612028.
  - [12] J. Preskill, Proc. R. Soc. Lond. A **454**, 385 (1998).
  - [13] A. Steane, Nature **399**, 124 (1999).
  - [14] D. Gottesman and I. L. Chuang, Nature **402**, 390 (1999).
  - [15] D. Gottesman and J. Preskill (1999), unpublished analysis of the accuracy threshold.
  - [16] E. Knill, R. Laflamme, and G. Milburn, Nature **409**, 46 (2001).
  - [17] T. E. Panel, Tech. Rep. LAUR-02-6900, Los Alamos National Laboratory (2002), produced for ARDA.
  - [18] D. Aharonov (2002), talk at QIP, IBM, Jan 16, 2002.
  - [19] W. Dür and H.-J. Briegel, Phys. Rev. Lett. **90**, 067901/1 (2003).
  - [20] A. M. Steane, Phys. Rev. A **68**, 042322/1 (2003).
  - [21] A. M. Steane (2002), quant-ph/0202036.
  - [22] A. M. Steane and B. Ibinson (2003), quant-ph/0311014.
  - [23] E. Knill, R. Laflamme, A. Ashikhmin, H. Barnum, L. Viola, and W. Zurek, LA Science **27**, 188 (2002), quant-ph/0207170.
  - [24] B. M. Terhal and G. Burkard (2004), quant-ph/04020104.
  - [25] R. Alicki (2004), quant-ph/0402139.
  - [26] C. H. Bennett, D. P. DiVincenzo, J. A. Smolin, and W. K. Wootters, Phys. Rev. A **54**, 3824 (1996).
  - [27] D. Gottesman, Ph.D. thesis, Calif. Inst. Tech, Pasadena, California (1997).
  - [28] C. H. Bennett, G. Brassard, S. Popescu, B. Schumacher, J. A. Smolin, and W. K. Wootters, Phys. Rev. Lett. **76**, 722 (1996), see also Erratum [32].

- [29] A. Steane, Fort. Phys. **46**, 443 (1998).
- [30] S. Bravyi and A. Kitaev (2004), quant-ph/0403025.
- [31] D. DiVincenzo, Fort. Phys. **48**, 771 (2000).
- [32] C. H. Bennett, G. Brassard, S. Popescu, B. Schumacher, J. A. Smolin, and W. K. Wootters, Phys. Rev. Lett. **78**, 2031 (1996).